**Supplementary Material (ESI) for Journal of Material Chemistry A**



---

## Electronic Supplementary Information

# Hydrothermal preparation of nitrogen, boron co-doped curved graphene nanoribbons with high dopant amounts for high-performance lithium sulfur battery cathodes

*Liang Chen [a], Jianrui Feng [b], Haihui Zhou[*a], Chaopeng Fu[*a], Guichang Wang [b], Liming Yang [a], Chenxi Xu [a], Zhongxue Chen [c], Wenji Yang [a] and Yafei Kuang[*a]*

[a]*State Key Laboratory for Chemo/Biosensing and Chemometrics, College of Chemistry and Chemical Engineering, Hunan University, Changsha, 410082, PR China*

[b]*Department of Chemistry, Key Laboratory of Advanced Energy Materials Chemistry (Ministry of Education) and Synergetic Innovation Center of Chemical Science and Engineering (Tianjin), Nankai University, Tianjin, 300071, PR China*

[c]*School of Power and Mechanical Engineering, Wuhan University, Wuhan, 430072, China*

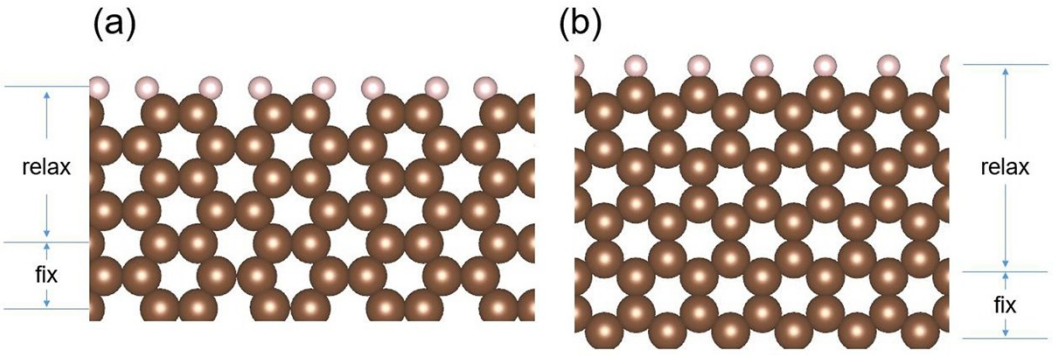


**Fig.S1** (a) Armchair and (b) zigzag model used for calculations, which adopt slab model to simulated edge of graphene. Fixed section was regarded as inner graphene sheet and relax section was used for investigating properties such as cohesive energy and binding energy of $Li_2S_x$

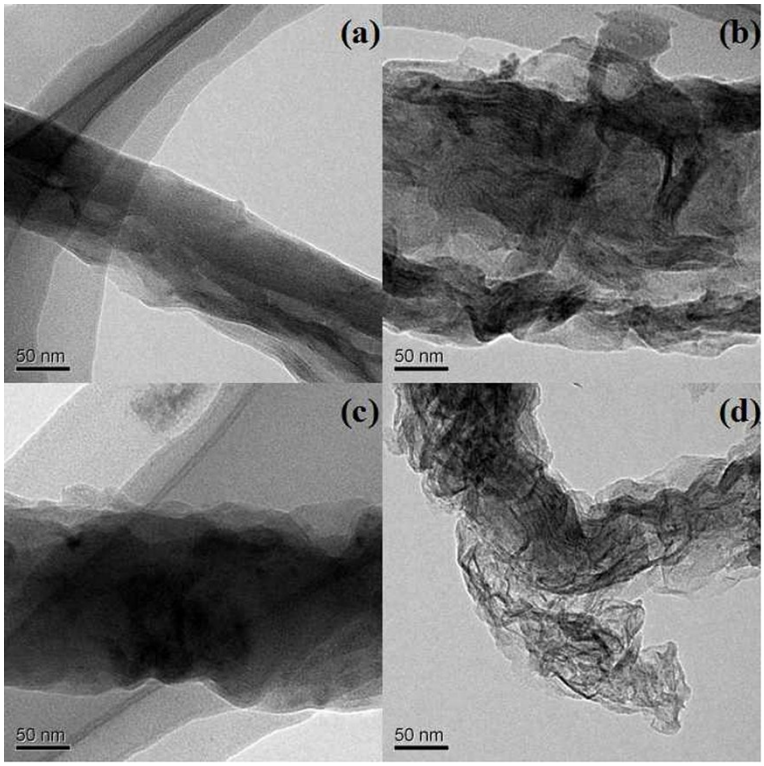


**Fig.S2** TEM images of CGN (a), NCGN (b), BCGN (c) and NBCGN (d)

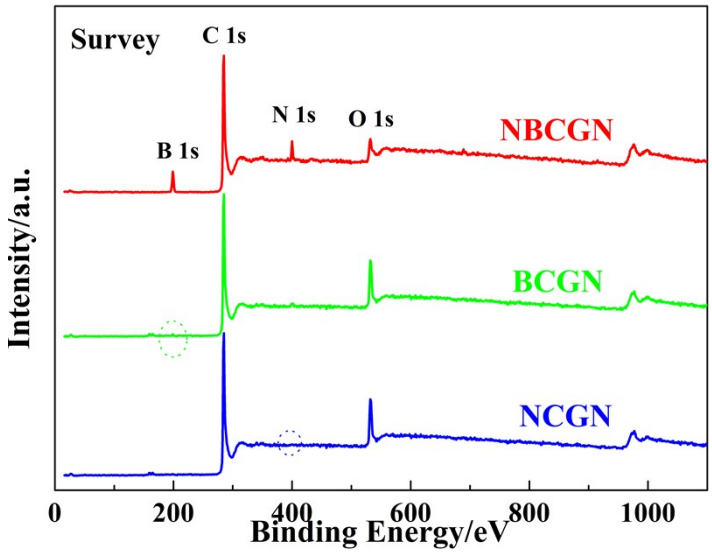


**Fig.S3** XPS survey spectra of NCGN, BCGN and NBCGN

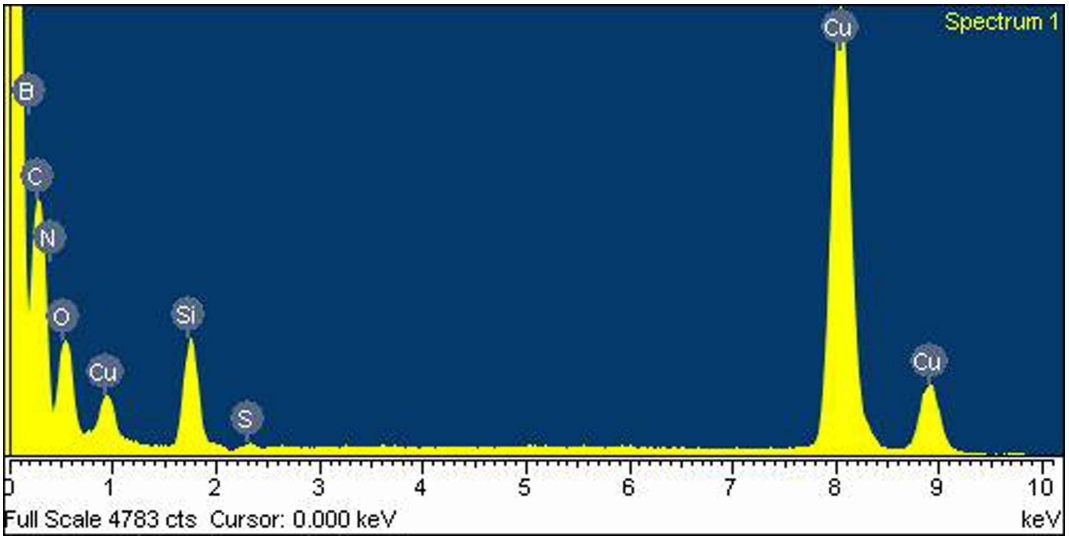


**Fig.S4** EDS spectrum of the NBCGN/S composite

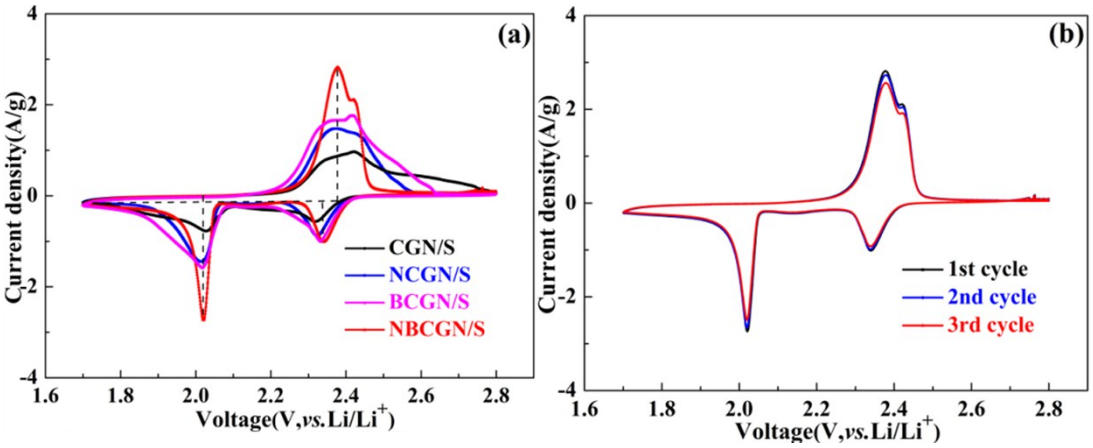


**Fig.S5** (a) CV curves of the CGN/S, NCGN/S, BCGN/S and NBCGN/S cathodes at 0.1 mV/s at the first cycle; (b) CV curves of the NBCGN/S cathode at a scan rate of 0.1 mV/s at the first three cycles

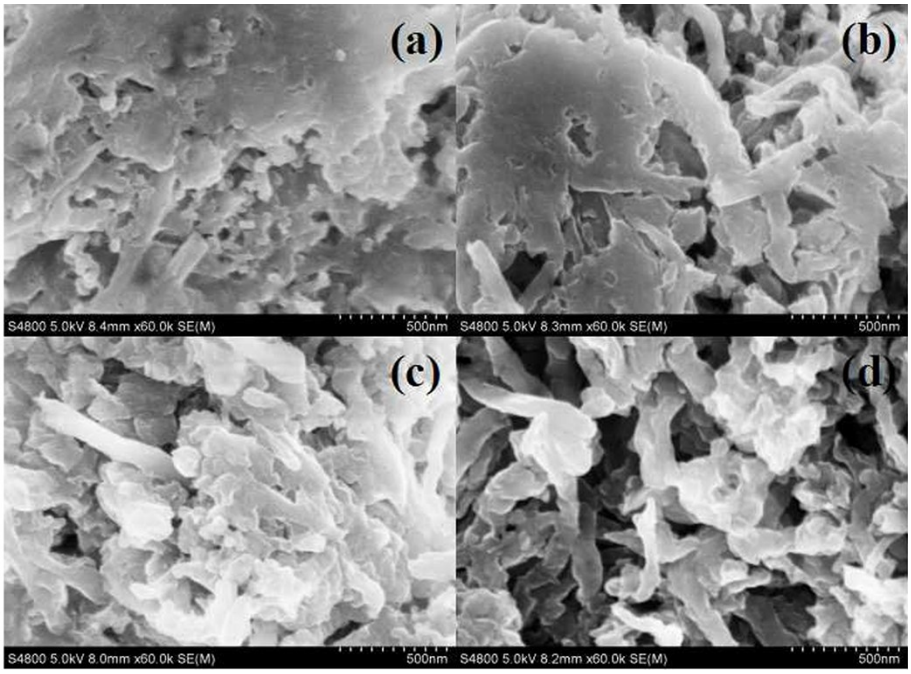


**Fig.S6** SEM images of CGN/S (a), NCGN/S (b), BCGN/S (c) and NBCGN/S (d) cathodes after 300 cycles at 0.2 C

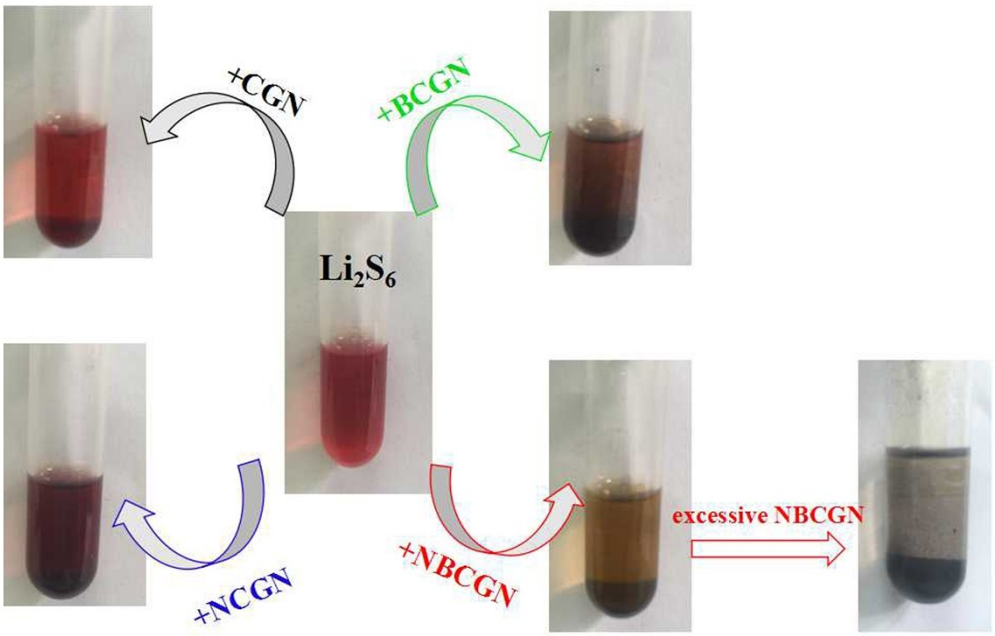


**Fig.S7** Visualized adsorption experiments for CGN, NCGN, BCGN and NBCGN in $Li_2S_6$ solution

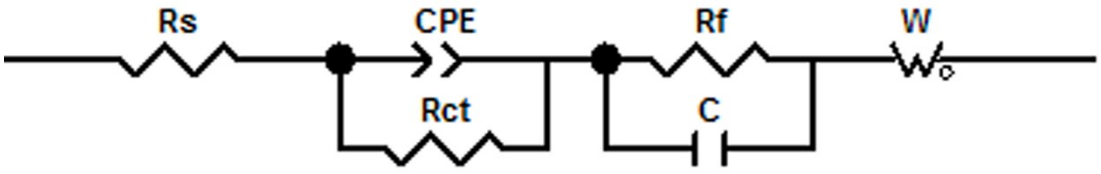


**Fig.S8** Equivalent circuit used for fitting the impedance data

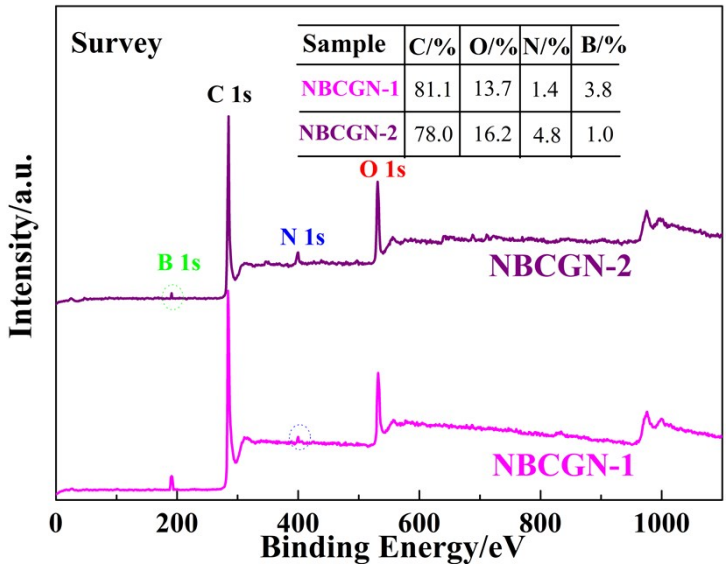


| Sample | C/% | O/% | N/% | B/% |
|---|---|---|---|---|
| NBCGN-1 | 81.1 | 13.7 | 1.4 | 3.8 |
| NBCGN-2 | 78.0 | 16.2 | 4.8 | 1.0 |

**Fig.S9** XPS survey spectra of NBCGN-1 and NBCGN-2

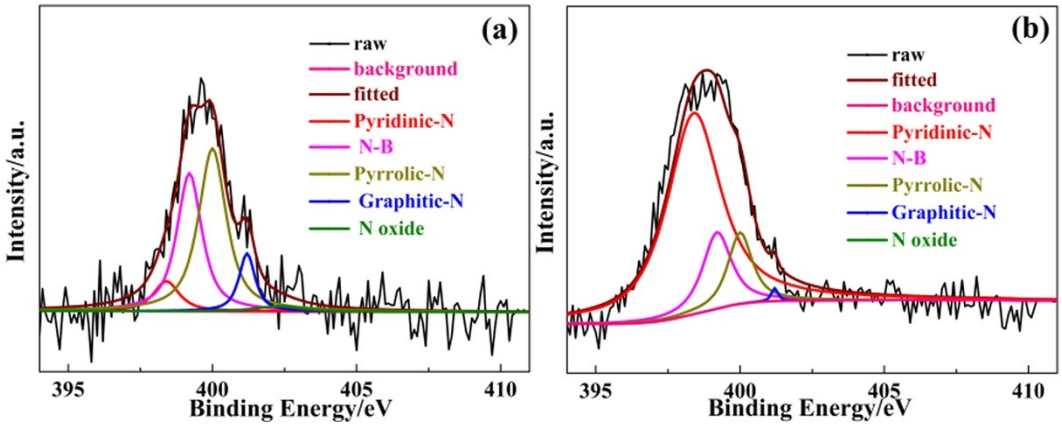


**Fig.S10** High resolution N 1s spectra of NBCGN-1 and NBCGN-2

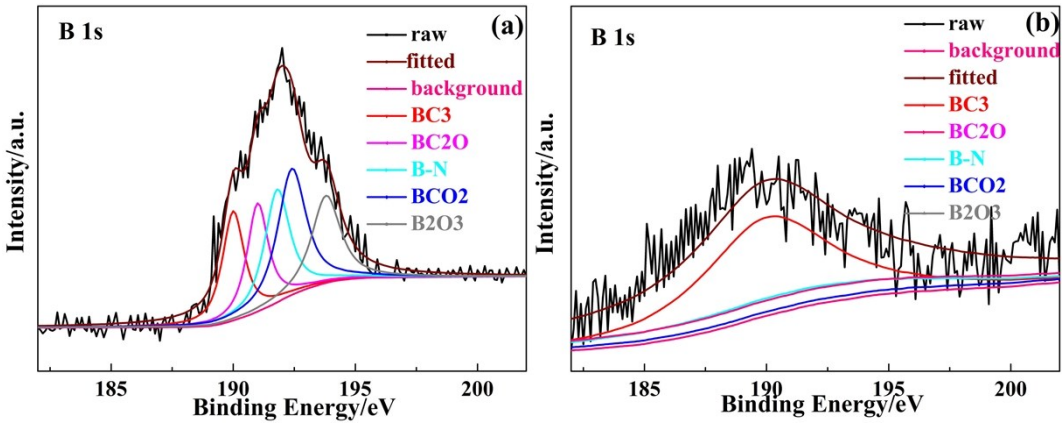


**Fig.S11** High resolution B 1s spectra of NBCGN-1 and NBCGN-2

**Table S1** BET specific surface area and pore volume of the CGN, NCGN, BCGN and NBCGN

| Sample | specific surface area/($m^2$/g) | total pore volume/($cm^3$/g) |
|---|---|---|
| CGN | 112.1 | 0.192 |
| NCGN | 147.1 | 0.215 |
| BCGN | 132.9 | 0.213 |
| NBCGN | 243.8 | 0.314 |

**Table S2** The specific N and B distributions in NCGN, BCGN and NBCGN. N-1 to N-5 represent pyridinic N, pyrolic N, graphitic N, oxygenated N and N-B, respectively; B-1 to B-5 stand for $BC_3$, $BC_2O$, $BCO_2$, $B_2O_3$ and B-N, respectively.

| sample | N distribution/at.% | | | | | B distribution/at.% | | | | |
|---|---|---|---|---|---|---|---|---|---|---|
| | N-1 | N-2 | N-3 | N-4 | N-5 | B-1 | B-2 | B-3 | B-4 | B-5 |
| NCGN | 19.1 | 20.6 | 17.9 | 42.4 | – | – | – | – | – | – |
| BCGN | – | – | – | – | – | 49.1 | 15.9 | 33.9 | 1.1 | – |
| NBCGN | 36.0 | 0.0 | 14.1 | 7.8 | 42.1 | 0.0 | 35.2 | 17.1 | 7.7 | 40.0 |

**Table S3** Comparison of the sulfur cathode performance between this work and some other works reported previously

| Samples | Sulfur loading mg/cm$^2$ | Current density | Initial capacity | Capacity loss rate per cycle | Reference |
|---|---|---|---|---|---|
| **NBCGN/S** | ~2.0 | **0.2C** | **977** | **0.08%** | **This work** |
| N-CNTs/S | ~0.55 | 0.2 C | ~800 | 0.18% | S1 |
| NG-S90 | ~1.5 | ~0.5C | 1080 | 0.11% | S2 |
| S@NG | 0.8 | 0.5 C | 1030 | 0.10% | S3 |
| 3D-NGS | ~1.0 | ~0.15C | ~1050 | 0.13% | S4 |
| Aligned CNTs/S | ~1.2 | 0.1C | 736 | 0.96% | S5 |
| HMMCNTs/S | 0.8-1.0 | ~0.3C | 1008 | 0.26% | S6 |
| Gr/CNTs | ~1.2 | 0.3C | 946 | 0.26% | S7 |
| G-NBCL400/S | 0.9-1.2 | 0.5C | 829 | 0.08% | S8 |
| HCNF@NPC-S | 1.8-2.5 | 0.5C | 1170 | 0.27% | S9 |
| MPNC-S80 | ~1.1 | ~0.1C | 1013 | 0.40% | S10 |

**Table S4** Impedance values of the equivalent circuit fitted for the impedance spectra

| Sample | $R_s$ | CPE-T | CPE-P | $R_{ct}$ | $R_f$ | $C$ |
|---|---|---|---|---|---|---|
| CGN/S | 1.94 | 1.12E-5 | 0.86 | 58.04 | 13.62 | 0.0019 |
| NCGN/S | 2.11 | 2.12E-5 | 0.76 | 51.44 | 13.09 | 0.00078 |
| BCGN/S | 1.92 | 8.57E-6 | 0.87 | 46.67 | 13.01 | 0.00020 |
| NBCGN/S | 1.91 | 6.52E-6 | 0.86 | 38.47 | 7.758 | 0.00089 |

**Table S5** The specific N distributions in NBCGN-1 and NBCGN-2. N-1 to N-5 represent pyridinic N, pyrolic N, graphitic N, oxygenated N and N-B, respectively;respectively; B-1 to B-5 stand for $BC_3$, $BC_2O$, $BCO_2$, $B_2O_3$ and B-N, respectively.

| sample | N distribution/at.% | | | | | B distribution/at.% | | | | |
|---|---|---|---|---|---|---|---|---|---|---|
| | N-1 | N-2 | N-3 | N-4 | N-5 | B-1 | B-2 | B-3 | B-4 | B-5 |
| NBCGN-1 | 7.7 | 45.7 | 9.4 | 2.5 | 34.7 | 17.5 | 16.9 | 18.4 | 26.2 | 21.0 |
| NBCGN-2 | 72.8 | 11.7 | 0.8 | 0 | 14.7 | 42.2 | 20.7 | 0.2 | 10.2 | 26.7 |

**Table S6** Calculated details of cohesive energy of each model. $E_c$, $E_{XX}$ and $E$(X) stand for cohesive energy, energy of X system and energy of the X atom.

| Systems | Formula to calculate $E_c$ | $E_c$ (eV) |
|---|---|---|
| CC | $E_{c,CC} = E_{CC} - E_{CC}$ | 0.00 |
| BC | $E_{c,BC} = E_{BC} - E_{CC} + E(B) - E(C) - E(H)$ | 4.69 |
| NC | $E_{c,NC} = E_{NC} - E_{CC} + E(N) - E(C) - E(H)$ | 2.60 |
| BC+NC | $E_{c,BC} + E_{c,NC}$ | 7.29 |
| BN | $E_{c,BN} = E_{BN} - E_{CC} + E(B) + E(N) - 2E(C) - 2E(H)$ | 6.16 |
| CCC | $E_{c,CCC} = E_{CCC} - E_{CCC}$ | 0.00 |
| BCC | $E_{c,BC} = E_{BC} - E_{CCC} + E(B) - E(C) - E(H)$ | 4.62 |
| NCC | $E_{c,NCC} = E_{NCC} - E_{CCC} + E(N) - E(C) - E(H)$ | 2.79 |
| BCC+NCC | $E_{c,BCC} + E_{c,NCC}$ | 7.41 |
| BCN | $E_{c,BCN} = E_{BCN} - E_{CCC} + E(B) + E(N) - 2E(C) - 2E(H)$ | 7.34 |

## References


S1. Y. Li, R. Mi, S. Li, X. Liu, W. Ren, H. Liu, J. Mei and W. M. Lau, *Int. J. Hydrogen Energy*, 2014, **39**, 16073-16080.

S2. J. Song, Z. Yu, M. L. Gordin and D. Wang, *Nano Lett.*, 2016, **16**, 864-870.

S3. Y. Qiu, W. Li, W. Zhao, G. Li, Y. Hou, M. Liu, L. Zhou, F. Ye, H. Li, Z. Wei, S. Yang, W. Duan, Y. Ye, J. Guo and Y. Zhang, *Nano Lett.*, 2014, **14**, 4821-4827.

S4. C. Wang, K. Su, W. Wan, H. Guo, H. Zhou, J. Chen, X. Zhang, Y. Huang, *J. Mater. Chem. A*, 2014, **2**, 5018-5023.

S5. X. B. Cheng, J. Q. Huang, Q. Zhang, H. J. Peng, M. Q. Zhao, F. Wei, *Nano Energy*, 2014, **4**, 65-72.

S6. K. Mi, Y. Jiang, J. Feng, Y. Qian and S. Xiong, *Adv. Funct. Mater.*, 2016, **26**, 1571-1579.

S7. S. Niu, W. Lv, C. Zhang, Y. Shi, J. Zhao, B. Li, Q.-H. Yang and F. Kang, *J. Power Sources*, 2015, **295**, 182-189.

S8. S. Yuan, J. L. Bao, L. Wang, Y. Xia, D. G. Truhlar and Y. Wang, *Adv. Energy Mater.*, 2016, **6**, 1501733.

S9. Q. Li, Z. Zhang, Z. Guo, Y. Lai, K. Zhang and J. Li, *Carbon*, 2014, **78**, 1-9.

S10. J. Song, T. Xu, M. Gordin, P. Zhu, D. Lv, Y. Jiang, Y. Chen, Y. Duan, D. Wang, *Adv. Funct. Mater.*, 2014, **24**, 1243-1250.